Optics Letters

# Room temperature continuous-wave operated 2.0-W GaN-based ultraviolet laser diodes

Jing Yang,[1,2] De-Gang Zhao,[1,2,*] Zong-Shun Liu,[1] Baibin Wang,[1] Yu-Heng Zhang,[1] Zhen-Zhuo Zhang,[1] Ping Chen,[1] and Feng Liang[1]

[1]State Key Laboratory of Integrated Optoelectronics, Institute of Semiconductors, Chinese Academy of Sciences, Beijing, 100083, China
[2]School of Electronic, Electrical and Communication Engineering, University of Chinese Academy of Sciences, Beijing, 100049, China
*Corresponding author: dgzhao@red.semi.ac.cn

Received 26 January 2022; revised 19 February 2022; accepted 20 February 2022; posted 28 February 2022; published 23 March 2022

**Temperature characteristics of near-UV laser diodes (LDs) with a lasing wavelength of 384 nm are investigated. The characteristic temperature of threshold current ($T_0$) of the UV LDs is low. Thus, the performance of the UV LDs under continuous wave (CW) operation is not as good as under pulsed operation especially at a high injection current. In addition, it is found that self-heating is a key factor for CW characteristics of the UV LDs, where suppression of the self-heating by using thick waveguide layers can increase the critical current of thermal rollover of the UV LD's operation. A high CW output power of 2.0 W is achieved for an InGaN near-UV LD with the n-side down on a sub-mount, whose threshold current density is 1.27 kA/cm$^2$ and the highest wall plug efficiency (WPE) is approximately 15.9% at an injection current of 1.2 A.** 

https://doi.org/10.1364/OL.454340

Although AlGaN-based ultraviolet light-emitting diodes (UV LEDs) with emission wavelength as short as 211 nm have been realized [1], to date, due to their greater structural complexity, the commercially available UV laser diodes (LDs) are still mainly limited to emission wavelengths above 370 nm [2–5]. UV LDs are potential light sources of various applications such as materials processing and ultraviolet curing. For these applications, high-wattage class operation is required to obtain, for example, quick cuttings of thick metal and high UV curing speeds. However, the highest optical output power of a 375–380 nm GaN-based commercially produced LD is approximately 400 mW, which is fabricated by Nichia Corporation. The performance is lower than that of blue LDs [6,7]. Thus, an investigation on how to realize high output power UV LDs is very important. It is known that apart from the threshold current and slope efficiency (SE) of LDs, the catastrophic optical mirror degradation (COMD) at facets and thermal rollover phenomenon at high injection current are also limiting factors of their output power [8,9]. Enhancing the characteristic temperatures of the lasing threshold ($T_0$) and slope efficiency ($T_1$) are effective methods for increasing the critical current, where the thermal rollover phenomenon occurs and improves the performance of LDs under a CW high injection current [10,11]. However, it is found that the $T_0$ is predominantly related to the thermal escape of electrons from quantum wells (QWs), which depends critically on the QW depth [12]. Thus, compared with violet LDs, the $T_0$ of UV LDs should be lower. In this case, thermal management is more critical. In this work, we study the temperature characteristics of UV LDs with a lasing wavelength of 384 nm under CW operation, and it is found that a higher wall plug efficiency (WPE) of LDs and corresponding weak self-heating effect lead to a better performance of LDs at a high injection current.

Two LD structures A and B were grown on c-plane free-standing GaN substrates by metal organic chemical vapor deposition (MOCVD). TMGa/TEGa, TMAl, TMIn, and $NH_3$ were used as Ga, Al, In, and N sources, respectively. The LD structures consisted of a 2-μm-thick n-type GaN layer, a 500-nm n-type $Al_{0.07}Ga_{0.93}N$ cladding layer (CL) with an n-doping concentration of $3 \times 10^{18}$ cm$^{-3}$, an unintentionally doped GaN lower waveguide (LWG) layer, an unintentionally doped AlGaN/InGaN multi-quantum well (MQW) active region, an unintentionally doped GaN upper waveguide (UWG) layer, a 20-nm $Al_{0.2}Ga_{0.7}N$:Mg electron blocking layer (EBL) with p-doping concentration of $1 \times 10^{19}$ cm$^{-3}$, a 500-nm $Al_{0.07}Ga_{0.93}N$:Mg CL layer with p-doping concentration of $5 \times 10^{18}$ cm$^{-3}$, and a 20-nm GaN:Mg contact layer with p-doping concentration of $1 \times 10^{20}$ cm$^{-3}$. The structure of AlGaN/InGaN MQW consisted of three 10-nm un-doped $Al_{0.03}Ga_{0.97}N$ barriers and two 5-nm un-doped $In_{0.04}Ga_{0.96}N$ QWs. The thickness of both the GaN LWG and UWG layers was 80 nm for LD A and 120 nm for LD B.

After the growth of the epilayer, LD chip fabrication processes were implemented using standard optical lithography in combination with various etching techniques for forming a lateral waveguide and a lift-off process for p-contact metal patterning. The ridge size of the LDs was 15 μm × 1200 μm. The front and rear cleaved facets were coated with a reflectivity of 16% and 80%, respectively. Finally, the LD chips were mounted with the n-side down on an AlN sub-mount. Then the output power versus current ($P$–$I$) curves were recorded at room temperature (RT) using a calibrated Si detector under a pulsed operation or CW operation. The pulse width was 500 ns and the duty cycle was 0.05%. The temperature dependent $P$–$I$ curves were measured on a sample table with temperature control function, whose temperature changed from 25 to 70°C.

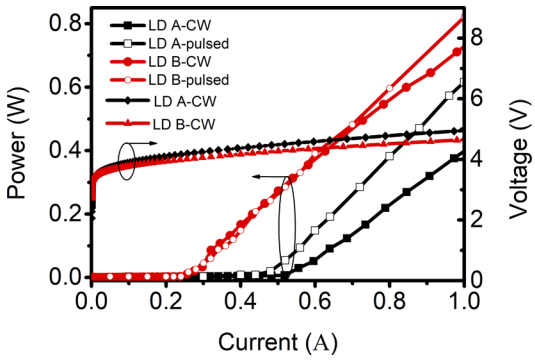


**Fig. 1.** *P–I* curves of LD A and LD B under pulsed (empty square and circle) and CW (solid square and circle) operation.

*P–I* characteristics were studied for LD A and LD B at RT. Figure 1 displays the *P–I* curves measured under pulsed and CW operation. The threshold current of LD B under pulsed operation was much lower than that of LD A, which was 460 mA (2.56 kA/cm$^2$) for LD A and 228 mA (1.27 kA/cm$^2$) for LD B. In addition, it is interesting to note that the CW characteristics were very different from those obtained under pulsed operation for both LD A and LD B. For LD A, the threshold current increased and the slope efficiency (SE) decreased under CW operation. However, for LD B, the threshold current and slope efficiency under CW operation were very similar to those under pulsed operation when the injection current was lower than 0.7 A. The slope efficiency started to slightly decrease only when the injection current was further increased.

It is well known that the deterioration of CW characteristic is always related to the poor thermal characteristics and the increased junction temperature of LDs. Therefore, the temperature-dependent *P–I* curves under pulsed operation were examined first to obtain the characteristic temperature ($T_0$) of the lasing threshold. Figures 2(a) and 2(b) show the pulsed *P–I* curves of LD A and LD B, respectively, as a function of temperature. The threshold current ($I_{th}$) increased and the slope efficiency slightly decreased when the temperature was increased from 30°C to 70°C. The relationship of ln($I_{th}$) with the temperature ($T$) was derived and fitted by using a linear relation for both LDs, as shown in the inset of Figs. 2(a) and 2(b). The calculated characteristic temperature $T_0$ of LD A and LD B was 139 K and 138 K according to the previously reported method [11,13], respectively. Therefore, the temperature characteristics of LD B were close to those of LD A. In addition, it is noted that the characteristic temperature $T_0$ for UV LD A and LD B was much lower than those of conventional violet LDs. It suggests that the variation of junction temperature may be a more important problem for the CW performance of UV LDs.

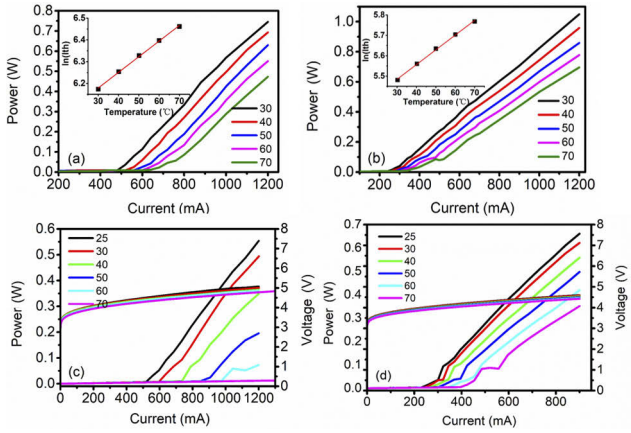


**Fig. 2.** Pulsed light output power versus injection current of (a) LD A and (b) LD B as function of temperature. Temperature dependences of CW *P–I–V* characteristics of (c) LD A and (d) LD B. The insets of (a) and (b) show ln($I_{th}$) as a function of temperature for LD A and LD B, respectively.

However, under CW operation, the dependence of output power on temperature was very different for LD A and LD B. For LD A, its $I_{th}$ increased and SE decreased quickly with increasing temperature, and it did not lase even though the injection current was increased to 1.4 A at a temperature of 70°C. For LD B, the $I_{th}$ increased and SE decreased much lower than those of LD A, and $I_{th}$ increased to only 150 mA for LD B when the measured temperature was increased from 25°C to 70°C. The output power of LD A deteriorated more than that of LD B with temperature, which indicated that the junction temperature of LD A is higher than that of LD B under CW operation. It may be due to the strong self-heating effect of LD A. In addition, there were obvious small kinks in the *P–I* curves for both LD A and LD B, which indicated that mode hopping occurs when the injection current increases, although the reason is not very clear currently.

In fact, the dependence of voltage value on temperature can be advantageously used for an exact determination of the junction temperature [14]. To check the junction temperature of LD A and LD B, CW *I-V* curves at different temperature were measured, as shown in Figs. 2(c) and 2(d). The voltage values of LD A and LD B at an injection current of 900 mA under different temperatures were extracted and are shown in Fig. 3(a). The voltage decreased from 4.9 V@25°C to 4.61 V@70°C for LD A, and it decreased from 4.6 V@25°C to 4.42 V@70°C for LD B. The decrease of voltage with increasing temperature of LD A was larger than that of LD B. It is known that the decreases of voltage with increasing temperature for GaN diode devices mainly results from the temperature-dependent increase of the hole concentration in Mg-doped AlGaN [15,16]. Thus, a larger variation of voltage value for LD A indicates a higher junction temperature, i.e., the self-heating effect of LD A is more serious than that of LD B. Such a self-heating effect also can be verified from the result of variation of lasing wavelength between pulsed operation and CW operation, as shown in Fig. 3(b). The lasing wavelength at the injection current of 1.2$I_{th}$ changed from 381.6 to 384.1 nm for LD A, which is an increase of 2.5 nm, but the increase was only 0.9 nm for LD B, i.e., it changed from 383 nm to 383.9 nm. It indicated that the increase of the junction temperature for LD B is less than that of LD A. The self-heating was much weaker for LD B under CW operation.

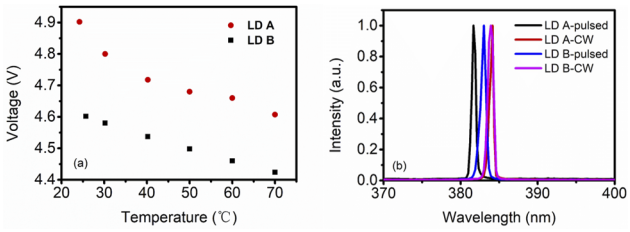


**Fig. 3.** (a) Temperature dependence of voltage value at an injection current of 900 mA under CW operation. (b) RT lasing spectra of LD A and LD B at an injection current of 1.2$I_{th}$ under pulsed and CW operation.

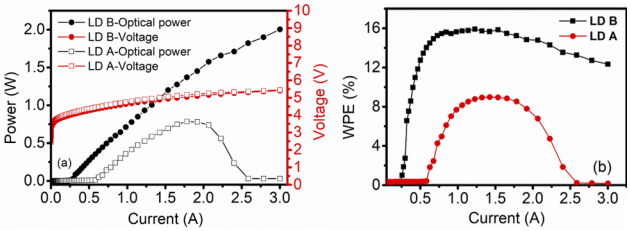


**Fig. 4.** (a) *P–I–V* curves of LD A and LD B under CW operation, and (b) wall plug efficiency versus current for LD A and LD B.

To investigate the self-heating effect on the performance of the LDs further, the *P–I–V* curves of LD A and LD B were measured at a large injection current of 3 A, and the corresponding WPE was also calculated. Both curves are shown in Fig. 4. The output power decreased when the injection current increased to higher than 1.9 A for LD A, and such a phenomenon was not observed for LD B until 3 A. The reduction of output power at high injection current may be caused by catastrophic optical mirror degradation (COMD) at facets or by the thermal rollover phenomenon. It is known that the reduction of output power caused by COMD is irreversible, but here the results of the *P–I–V* curve measurement were repeatable. Therefore, the thermal rollover phenomenon was responsible for our observed reduction of the output power for LD A. Based on the result of LD B, a UV LD with a large output power of 2.0 W was obtained at 3 A even though the flip chip package process was not used for accelerating the heat dissipation.

From Fig. 4(b), the WPE of LD B was much higher than that of LD A, and the highest WPE was approximately 15.9% at an injection current of 1.2 A for LD B. A higher WPE may be attributed to the thicker WG layers of LD B, which may result in a smaller optical absorption loss due to the decreased optical field penetration into doped n/p cladding layers [17]. To verify this speculation, the optical field distribution of LD A and LD B were theoretically simulated by the Crosslight Device Simulation Software (LASTIP, Crosslight Software Inc.), where the absorption coefficients of n-type and p-type layers were set as 10 $cm^{-1}$ and 50 $cm^{-1}$, respectively, except for the heavily Mg-doped GaN contact layer, whose absorption coefficient was taken as 100 $cm^{-1}$. The optical confinement factor and absorption loss of the LDs were calculated according to their optical field distribution, and they were 4.76%, 10.9 $cm^{-1}$ and 4.7%, 8.02 $cm^{-1}$ for LD A and LD B, respectively. It indicates that the optical absorption loss of LD B was much lower than that of LD A. It agrees well with the experimental results that the threshold current of LD B is much lower than that of LD A. In addition, the small absorption loss of LD B leads to a lower amount of the heat generated in the process of lasing, and therefore, higher WPE and output power are obtained for LD B. However, the AlN mole fraction of the n-AlGaN CL layer is relatively high for UV LDs, which results in a large strain and rough surface. Therefore, a thicker GaN WG layer is beneficial for reducing strain and recovering the surface quality. In this case, the material quality of an MQW active region grown on a thick GaN WG layer should be improved. Thus, a good material quality of the MQW active region may be also responsible for the excellent characteristic of LD B.

The performance of high output power UV LDs with different thicknesses of GaN waveguide layers was investigated. It is interesting to note that the performance with thinner WG layers was not as good as that with thicker WG layers, especially at a high injection current and under the CW operation. The improvement of performance was attributed to the weaker absorption loss for LDs with thicker WG layers, and the consequent weaker self-heating effect. Finally, a high CW output power of 2.0 W at a wavelength of 384 nm for a single InGaN UV LD was achieved, its threshold current density was 1.27 $kA/cm^2$, and the highest WPE was approximately15.9% at an injection current of 1.2 A.

**Funding.** National Key Research and Development Program of China (2021YFF0307403); National Natural Science Foundation of China (61874175, 61904172, 61974162, 62034008, 62074140, 62074142); Youth Innovation Promotion Association of the Chinese Academy of Sciences (2019115); Beijing Nova Program (202093); Strategic Priority Research Program of Chinese Academy of Sciences (XDB43030101).

**Disclosures.** The authors declare no conflicts of interest.

**Data availability.** Data underlying the results presented in this paper are not publicly available at this time but may be obtained from the authors upon reasonable request.

## REFERENCES

1. Y. Taniyasu and M. Kasu, Appl. Phys. Lett. **96**, 221110 (2010).
2. https://www.nichia.co.jp/cn/product/laser.html
3. J. Yang, D. G. Zhao, Z. S. Liu, F. Liang, P. Chen, L. H. Duan, H. Wang, and Y. S. Shi, J. Semicond. **43**, 010501 (2022).
4. H. Amano, R. Collazo, and C. D. Santi, *et al.*, J. Phys. D: Appl. Phys. **53**, 503001 (2020).
5. Y. Nakatsu, Y. Nagao, K. Kozuru, T. Hirao, E. Okahisa, S. Masui, T. Yanamoto, and S. Nagahama, Proc. SPIE **10918**, 109181D (2019).
6. F. Liang, D. G. Zhao, Z. S. Liu, P. Chen, J. Yang, L. H. Duan, Y. S. Shi, and H. Wang, J. Semicond. **42**, 112801 (2021).
7. M. Kawaguchi, O. Imafuji, S. H. Nozaki, H. Hagino, S. Takigawa, T. Katayama, and T. Tanaka, Proc. SPIE **9748**, 974818 (2016).
8. Y. C. Wang, A. Y. Qi, Y. F. Wang, H. W. Qu, and W. H. Zheng, Electron. Lett. **57**, 564 (2021).
9. Z. Q. Ren, Q. M. Li, B. Li, and K. C. Song, J. Semicond. **41**, 032901 (2020).
10. C. E. Zah, R. Bhat, B. N. Pathak, and J. J. Hsieh, IEEE J. Quantum Electron. **30**, 511 (1994).
11. D. Sizov, R. Bhat, K. Song, D. Allen, and C. E. Zah, Appl. Phys. Express **4**, 102103 (2011).
12. A. Bojarska, J. Goss, L. Marona, A. Kafar, S. Stanczyk, I. Makarowa, S. Najda, G. Targowski, T. Suski, and P. Perlin, Appl. Phys. Lett. **103**, 071102 (2013).
13. P. Y. Wen, S. M. Zhang, D. Y. Li, J. P. Liu, L. Q. Zhang, X. J. Su, K. Zhou, A. Q. Tian, C. Zeng, D. S. Jiang, Z. S. Liu, and H. Yang, Semicond. Sci. Technol. **30**, 125015 (2015).
14. H. Y. Ryu, K. H. Ha, J. H. Chae, O. H. Nam, and Y. J. Park, Proc. SPIE **5738**, 1 (2005).
15. P. Kozodoy, Y. P. Smorchkova, M. Hansen, H. Xing, S. P. DenBaars, U. K. Mishra, A. W. Saxler, R. Perrin, and W. C. Mitchel, Appl. Phys. Lett. **75**, 2444 (1999).
16. M. Z. Kauser, A. Osinsky, A. M. Dabiran, and P. P. Chow, Appl. Phys. Lett. **85**, 5275 (2004).
17. J. Yang, B. B. Wang, D. G. Zhao, Z. S. Liu, F. Liang, P. Chen, Y. H. Zhang, and Z. Z. Zhang, J. Appl. Phys. **130**, 173105 (2021).